ISSN 1068-3755, Surface Engineering and Applied Electrochemistry, 2019, Vol. 55, No. 1, pp. 46–52. © Allerton Press, Inc., 2019.
Russian Text © S.S. Belevskii, A.V. Gotelyak, S.A. Silkin, A.I. Dikusar, 2018, published in Elektronnaya Obrabotka Materialov, 2018, No. 2, pp. 9–15.

Macroscopic Size Effect on the Microhardness of Electroplated Iron Group Metal–Tungsten Alloy Coatings: Impact of Electrode Potential and Oxygen-Containing Impurities

S. S. Belevskii[a], A. V. Gotelyak[b], S. A. Silkin[b, c], and A. I. Dikusar[a, b, *]

[a] *Institute of Applied Physics, Academy of Sciences of Moldova, Chisinau, MD-2028 Moldova*
[b] *Shevchenko Pridnestrovie State University, Tiraspol, MD-3300 Moldova*
[c] *Kostroma State University, Kostroma, 156005 Russia*
**e-mail: dikusar@phys.asm.md*

Received December 19, 2017; revised February 14, 2018

Abstract—The cause of the microscopic size effect in the microhardness of electroplated binary alloys between iron group metals and tungsten is identified by studying electrodeposition of Co–W alloys. The effect is caused by the presence of oxygen-containing impurities in electroplated alloys, the impurity content growing with increasing the volume current density, which leads to a reduction in the coating microhardness. We find that the nature of anodes used affects the properties of deposited coatings, in particular, microhardness, because a deposition-inducing metal complex, which is a complex of an iron group metal, is consumed during electrolysis not only at the cathode, but it may also undergo oxidation at the anode, which identifies the way the anode affects the coating properties.

Keywords: electroplated coatings, alloys between iron group metals and tungsten, microhardness, induced codeposition, volume current density

DOI: 10.3103/S1068375519010058

Earlier studies have identified that electrodeposition of alloys between the iron group metals and tungsten (i.e., Fe–W, Ni–W, and Co–W) from citrate- and gluconate-containing baths produces coatings for which a microscopic size effect in microhardness (and probably other properties) can be observed [1–3]. With this effect present, the characteristics of coating, in particular, its microhardness, depend on the deposition surface area, apart from the bath composition, temperature, pH, and applied current density. This implies that this property (microhardness) is controlled by volume current density (VCD or I_v in figures), in addition to other ways known in electrochemistry, since the VCD can be raised by increasing the deposition surface area while keeping the applied current density and the electrolyte volume at the same level.

The electrodeposition of such alloys is classified as induced codeposition because the classical theory of alloy electrodeposition fails to predict alloy composition in such cases [4, 5]. In this respect, the process may be considered anomalous [5]. For instance, tungsten cannot be electrodeposited from aqueous media, but if a complex of an iron group metal (deposition-inducing metal) is added to the electrolyte a considerable tungsten content will be found in produced alloy coating.

As was established previously, the effect in question was characteristic of electrodeposition of binary iron group metals–tungsten alloys, i.e., under the conditions of induced codeposition, and it was not identified in classical processes such as chromium electrodeposition from the standard bath or nickel from the Watt's electrolyte. Additionally, it was found that at a fixed deposition current density the coating microhardness can be controlled by varying not only the deposition surface area, but the bath volume as well, with the current density and the deposition surface area held constant in this latter case. The findings reported in works [1–3] suggest that the VCD does not affect the components constituting the metal part of deposited alloy, i.e., the ratio between W and the iron group metal used, but the structure and morphology of the deposited coating are affected (clearly, the changes in morphology echoed the induced structural modifications). The findings of the works just cited, however, did not elaborate on the possible nature of the considered effects. To date, this has been only an experimental observation.

In electrochemical settings, changes to the structure of a coating are typically consequent to a change in the electrodeposition potential [6]. In the works cited above [1–3], electrodeposition was conducted

Table 1. The microhardness of coatings obtained at an applied current density of 2 A/dm^2 and the respective electrodeposition potentials

Entry no.	S, cm^2	HV, kgf/mm^2	I_v, mA/L	E_{meas}, V	ΔE_{IR}, V	E_{calc}, V
1	1	889 ± 12	6.7	–0.96	0.07	–0.89
2	2	833 ± 19	13.4	–0.99	0.1	–0.89
3	5	804 ± 24	33.5	–1.09	0.2	–0.89
4	10	697 ± 17	67.5	–1.14	0.24	–0.9

under galvanostatic conditions, i.e., the electrode potential was not controlled. Moreover, the observed effects were undoubtedly rooted in the mechanism of the induced codeposition of the iron group metals with tungsten, which to this day remains the subject of debate [4, 5, 7–12]. The aim of the present work is to identify the role that electrode potential plays in the electrodeposition of the group of alloys being considered and establish the mechanism of induced codeposition that would be adequate to the experimental observations.

EXPERIMENTAL

Electrochemical measurements were performed using a PARSTAT 2273 potentiostat, controlled by the software Power Suite, v. 2.58. The potentials were measured relative to a saturated Ag/AgCl electrode.

Electrodeposition was carried out in a 3 L cell at a temperature of 80°C in the galvanostatic mode at a current density of 2 A/dm^2 from a bath containing $CoSO_4$ (0.053 M), Na_2WO_4 (0.05 M), sodium gluconate ($C_6H_{11}NaO_7$; 0.55 M), H_3BO_3 (0.65 M), and NaCl (0.51 M); the pH was 6.5. In electrodeposition experiments, the VCD, defined as I/V, where I is the current and V is the bath volume, was varied from 6.7 to 67.5 mA/L. The substrates were St20 stainless steel plates with surface areas of 1, 2, 5, and 10 cm^2 (the other side was isolated from the electrolyte). Variation of the VCD was achieved by varying the surface area of the electrodeposition at a constant current density and bath volume. Because for a given bath volume, variation in the VCD was necessarily accompanied by changes in the electrodeposition current, the ohmic drop component ΔE_{IR} of experimentally measured potential was different for different experiments. The ohmic drop was determined using electrochemical impedance spectroscopy, and the electrode potentials measured at in experiments with different VCDs were corrected for ΔE_{IR}.

Prior to every electrodeposition experiment, the substrate was coated with a nickel layer. Nickel electrodeposition was conducted in a bath containing $NiCl_2 \cdot 6H_2O$ (240 g/L) and concentrated HCl (80 g/L) at a current density of 3 A/dm^2 for 60 s, which nickel coatings with a thickness of ~0.5 μm. The duration of alloy electrodeposition was calculated so that a ~30 μm thick layer was produced.

The morphology and elemental composition of prepared coatings were investigated using a Hitachi TM3000 scanning electron microscope, and the chemical composition was analyzed using an EDS attachment to this instrument. The coating microhardness was measured using a PMT-3 microhardness tester. Indentations were made with a Vickers diamond indenter using an indenter load of 100 g. Each sample was measured at least three different points. The results of the measurements are presented as an average value with the corresponding standard deviation.

RESULTS AND DISCUSSION

Potential transients recorded during electrodeposition on substrates with different surface areas are shown in Fig. 1a, and the variation of coating microhardness with VCD for the same samples is given Fig. 1b. As is evident, the electrodeposition potential grew (shifted cathodically) as the VCD increased, which was to be expected, considering the changes in the ohmic drop component of the measured potential (see Table 1) with the raise in electrodeposition current at a fixed current density. However, with the ohmic drop taken into account, the electrode potential does not exhibit a variation with the VCD (Table 1). We note that the HV values reported here were less than those obtained in works [1–3] by 6–10%. This diminution can be explained by that the bath used in these series of depositions (series I) was not freshly prepared (before these experiments, the bath age Q was already ~2 A h/L), and the HV falls as Q increases, as was established, in particular, in works [1–3]. Actually, the observed diminution of 6–10% matches well with a bath age of ~2 A h/L [3].

Similar results were obtained in another series of electrodeposition experiments (series II), in which a freshly prepared bath was used (Fig. 1). That bath, however, was not conditioned long enough, which is an important factor, given that the microhardness of the coatings plated from a bath that had been conditioned for a few days was found to be higher than plating from a fresh bath [1]. It is clear that, irrespective of specific features of electrodeposition, the results are nearly identical—they agree well with those reported earlier [1–3]. We emphasize that the observed dimi-

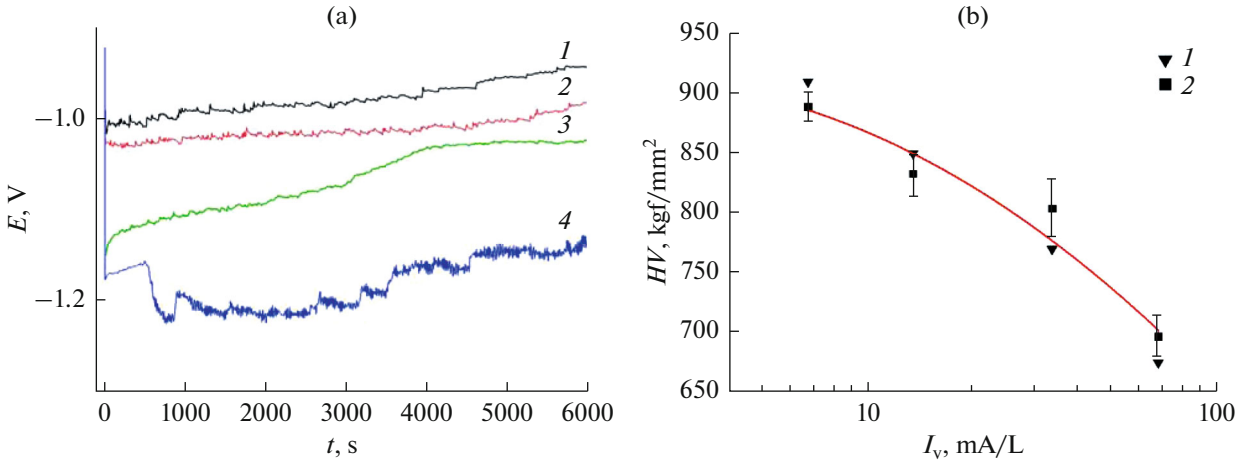

Fig. 1. (a) Potential transients during electroplating onto substrates with different surface areas: (*1*) 1, (*2*) 2, (*3*) 5, and (*4*) 10 cm^2. (b) The variation of microhardness of the electroplated coatings with VCD for the experiments of (*1*) series I and (*2*) series II.

nution in the microhardness with an increase in the VCD by ~30% is significantly greater than the relative standard deviation of the values obtained by averaging measurements made at different regions of a given electroplated coating (1–3%, see Table 1).

The most important conclusion that follows from the data presented in Fig. 1 and in Table 1 is that, despite the same values for electrode potential, the coating microhardness fell with the increasing VCD. This also means that the changes in microhardness described above that echoed the structural changes in the coatings were not related to changes in the electrode potential; instead, they were caused by processes in the bulk of electrolyte.

As was remarked earlier, the current efficiency of electrodeposition was not affected by VCD. Therefore, we can write

$$V_i = \frac{\Delta c}{\tau} = \frac{c_i - c_x}{\tau} = \frac{\Delta m}{V\tau} = \frac{CE\,C\,I}{V}, \qquad (1)$$

where Δc is the temporal variation of the solution concentration of the deposition-inducing metal species, Δm is the mass of plated metal coating, C is the electrochemical equivalent of the deposited alloy, I is the current, CE is the current efficiency, V is the bath volume, and τ is the deposition time.

As can be seen, different rates of change in the concentration of deposition-inducing metal species, which is a complex containing one of the iron group metals, is the underlying cause of changes in the VCD.

The results reported here for the electrodeposition of Co–W alloys from gluconate baths, can be rationalized in the framework of a mechanism proposed in [11, 12] (Fig. 2). The key feature of this mechanism is that the first stage in the formation of an alloy is electroreduction of the deposition-inducing metal species to form an intermediate (stage 1, Fig. 2). This stage was shown to be a slow one [11, 12]. This intermediate species is further reduced to a pure Co (stage (2), Fig. 2) or to form an alloy (stage (3), Fig. 2), this second route being mediated by the formation of a mixed metal cluster. In this cluster, the deposition-inducing metal is bonded to the refractory metal. Stages (2) and (3) are fast and, therefore, do not affect the electrode potential.

Electrodeposition under discussion does not necessarily proceeds through reactions (1)–(3). The intermediate species, in this case, it is $CoOH_{ads}$, may undergo chemical oxidation to form oxygen-containing impurities (oxides and hydroxides; reaction (4) in Fig. 2) [13]. In this case, hydrogen absorption by the coating may occur as well. Clearly, with this reaction

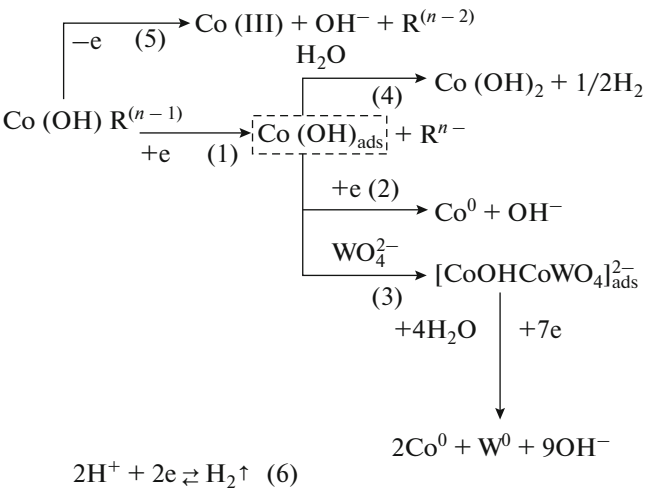

Fig. 2. Diagram of electrochemical processes occurring during electrodeposition of Co–W alloys.

branch included in the process, the microhardness of the coating will decrease.

This can be corroborated by the data given in Figs. 3 and 4. The micrographs of Fig. 3 adopted from work [3] show the surface of Co–W alloy coatings electroplated from a concentrated borate–gluconate bath (fivefold more concentrated in terms of metal components, the concentrations of other constitutes being the same) at different VCD and Q. It was found that the tungsten content of the metallic part of the coatings did not change when the VCD was increased [3]: in Fig. 3, panels a and b show two series of images corresponding to a low and a high VCD, respectively. On the other hand, the tungsten content increased considerably with Q, due to the fact that the solution concentration of W-containing species was falling slower than that of the deposition-inducing metal species. The data shown in Fig. 3 clearly shows us that, although the W content of the different coatings that remained the same as that of the VCD was increased, the morphology and, consequently, structure of the coatings underwent cardinal changes.

We found that in this case the oxygen content increased dramatically in uppermost layers of the deposited coatings, as can be appreciated from Fig. 4. The crucial effect the oxygen content of the deposited coatings has on their morphology (and structure) can be clearly seen by comparing the oxygen content and morphology of coatings obtained at the low and high VCDs and a high Q (10 A h/L). In this case, the coatings have nearly the same oxygen content (Fig. 4) and they thus have nearly identical morphologies (Fig. 3). It seems obvious that incorporation of oxygen-containing impurities in the coatings, their concentration being much higher at higher VCDs, is primarily responsible for the changes in their structure and thus in morphology.

The content of oxygen-containing impurities in the coatings grew with increasing the rate of consumption of deposition-inducing metal species in the bath, i.e., essentially with the VCD (see Eq. (1)). This feature, apart from manifesting during extended electroplating at both the low and high VCDs (Fig. 4), shows up as an effect of anodic processes (albeit to different extents) on the coating microhardness (Fig. 5). Assuming that changes in microhardness are related to increases in the content of oxygen-containing impurities in coatings, the effect the anode has on the microhardness during extended plating can apparently be attributed to the different rates of depletion of deposition-inducing metal species from the bath when different types of anodes are used. This in turn means that the depletion of the deposition-inducing complex species occurs in the anodic process, along with the cathodic one, put differently, the cobalt species may oxidize at the anode (reaction 5 in Fig. 2). At the same time, it implies that the oxidation rate of cobalt species is considerably higher at a platinum anode than at a graphite one (Fig. 5).

Clearly, the use of soluble anodes can be quite promising both in keeping the properties of the surface stable during extended electroplating and increasing the deposition rate, since in this case the possibility of having the deposition-inducing metal species oxidized at the anode is eliminated. For instance, this was demonstrated in work [2] in which a soluble tungsten anode was used in electroplating Co–W alloys. A more detailed discussion of the effects of anodic processes on the properties of electroplated coatings will be presented in a separate paper. The effects the anodic processes have on the deposition rate originate from that a hydrogen evolution reaction (reaction (6) in Fig. 2) may run parallel to reactions (1)–(5) (Fig. 2). With a decrease in the concentration of deposition-inducing metal species, the relative contribution of this reaction will rise.

We have thus presented a whole series of experimental evidence—independence of the electrode potential on the VCD, the effect of bath volume on microhardness at a fixed deposition current density, and the influence of anodic processes—suggesting that the observed effects are consequent to the processes in the bulk of electrolyte. The key question is why the VCD (i.e., essentially the rate of change in, most likely, the concentration of deposition-inducing metal species, but effects on other complex species cannot be excluded as well) has such a large impact on coating properties, in particular, on microhardness.

It seems obvious that the effect of oxygen-containing impurities incorporated in a coating affect its microhardness. However, one wonders as to the nature of the interrelationship between the VCD and the content of oxygen impurities in the coating. With the available experimental data, an exhaustive answer can hardly be provided. We must, however, take into consideration that the complex species involved have large molecular weights [14–16]. Additionally the formation of high molecular weight products is a slow process, hence the dependence of the bulk properties on time, which also manifests in effects on the mechanical properties of electroplated coatings [1, 16].

We highlight that accepting the mechanism of induced codeposition proposed in [11, 12] and complementing it with a hypothesis of the deposition-inducing metal species undergoing oxidation at the anode enabled a deeper understanding of the processes accompanying electroplating of the considered group of alloys. A number of experimental results presented herein can be considered as an indirect evidence supporting the correctness of the discussed mechanism of electrodeposition.

As for its application in technology, the results of our study (i) corroborate the important role the VCD

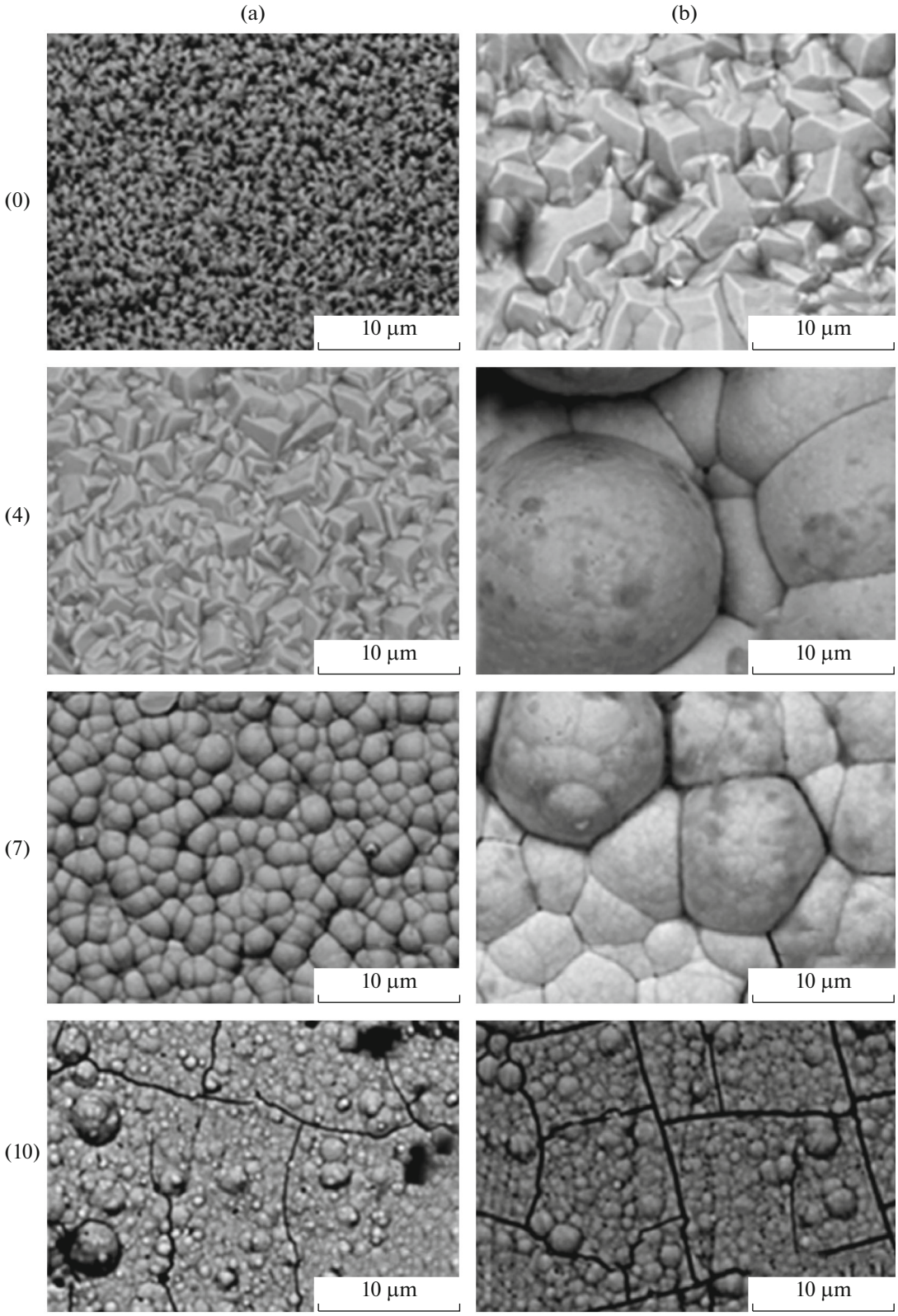

Fig. 3. The effect of the bath age on the coating morphology at a VCD of (a) 4 and (b) 400 mA/L. The numbers in the figures indicate the bath age in A h/L [3].

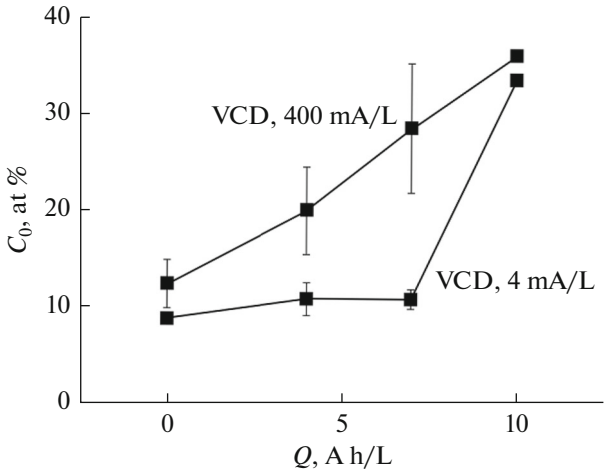

Fig. 4. Variation of the oxygen content in deposited coatings with electrodeposition time at different VCDs.

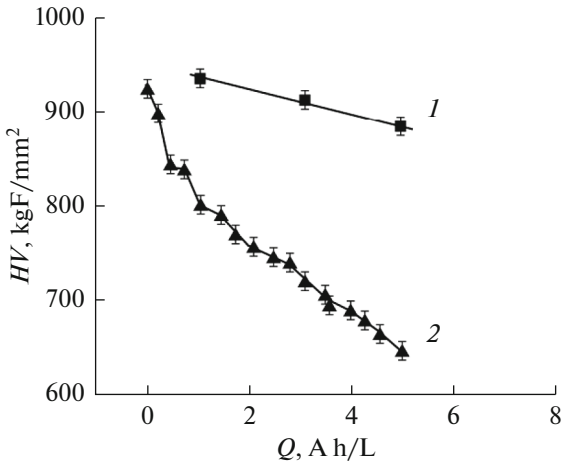

Fig. 5. Variations of the microhardness of Co–W alloys electroplated using (*1*) graphite and (*2*) platinum anodes; the VCD was 20 mA/L for both cases.

plays in controlling the surface properties of electroplated coatings and in scaling up the technology of these alloy coatings and (ii) demonstrate broad possibilities for controlling the deposition rate and coating properties by using different anodes, especially, soluble ones.

CONCLUSIONS

(1) For electrodeposition of Co–W alloys from a borate–gluconate bath, by way of example, we showed that with changing the VCD the alteration in the morphology and structure of alloy coatings obtained by the codeposition of iron group metals with tungsten is caused by the processes in the bulk of electrolyte, with the electrode potential remaining unaffected by increasing the VCD, while the surface morphology varies.

(2) The macroscopic size effect in coating microhardness (i.e., variation of microhardness with deposition surface area at a fixed applied current density (or potential)) is attributed to the incorporation of oxygen-containing impurities in the coating.

(3) The results are interpreted within a codeposition mechanism in which the first (limiting) stage is the reduction of deposition-inducing metal species (i.e., an iron group metal; here, Co) to an intermediate, followed by the reduction of the latter to a respective metal or alloy; alternatively, the intermediate may undergo chemical oxidation to form oxygen-containing impurities in the coating thereby reducing its microhardness.

(4) The deposition-inducing metal complex, along with being consumed at the cathode, is oxidized at the anode, which brings the nature of anode into picture and identifies the way the anode affects the coating properties.

CONCLUSIONS

This work was supported by the budget of the project "Physicochemical Methods for Obtaining New Materials and Surfaces for Multiscale Technologies" (no. 15.817.02.05A) of the Academy of Sciences of Moldova, the Europe-funded project "H2020 Smart-electrodes" (no. 778357), and the Shevchenko Pridnestrovie State University.

REFERENCES

1. Silkin, S.A., Gotelyak, A.V., Tsyntsaru, N.I., and Dikusar, A.I., *Surf. Eng. Appl. Electrochem.*, 2015, vol. 51, no. 3, pp. 228–234.
2. Belevskii, S.S., Bobanova, Zh.I., Buravets, V.A., et al., *Russ. J. Appl. Chem.*, 2016, vol. 89, no. 9, pp. 1427–1433.
3. Gotelyak, A.V., Silkin, S.A., Yahova, E.A., and Dikusar, A.I., *Russ. J. Appl. Chem.*, 2017, vol. 90, no. 4, pp. 541–546.
4. Podlaha, E.J. and Landolt, D., *J. Electrochem. Soc.*, 1996, vol. 143, no. 3, pp. 885–892.
5. Eliaz, N. and Gileadi, E., Induced codeposition of alloys of tungsten, molybdenum and rhenium with transition metals, in *Modern Aspects of Electrochemistry*, New York: Springer-Verlag, 2008, vol. 42, pp. 191–301.
6. Gamburg, Yu.D. and Zangari, G., *Theory and Practice of Metal Electrodeposition*, New York: Springer-Verlag, 2011.
7. Vas'ko, A.T., *Elektrokhimiya molibdena i vol'frama* (Electrochemistry of Molybdenum and Tungsten), Kiev: Naukova Dumka, 1977.

8. Podlaha, E.J. and Landolt, D., *J. Electrochem. Soc.*, 1997, vol. 144, no. 5, pp. 1672–1680.

9. Sun, S., Bairachna, T., and Podlaha, E.J., *J. Electrochem. Soc.*, 2013, vol. 160, no. 10, pp. D434–D440.

10. Tsyntsaru, N., Cesiulis, H., Donten, M., et al., *Surf. Eng. Appl. Electrochem.*, 2012, vol. 48, no. 5, pp. 491–520.

11. Krasikov, A.V. and Krasikov, V.L., *Izv. S.-Peterb. Gos. Tekhnol. Inst.*, 2016, no. 36 (62), pp. 12–23.

12. Krasikov, V.L. and Krasikov, A.V., *Izv. S.-Peterb. Gos. Tekhnol. Inst.*, 2016, no. 37, pp. 8–13.

13. Krasikov, V.L., *Izv. S.-Peterb. Gos. Tekhnol. Inst.*, 2015, no. 31, pp. 40–46.

14. Belevskii, S.S., Yushchenko, S.P., and Dikusar, A.I., *Surf. Eng. Appl. Electrochem.*, 2012, vol. 48, no. 1, pp. 97–98.

15. Shulman, A.I., Belevskii, S.S., Yushchenko, S.P., and Dikusar, A.I., *Surf. Eng. Appl. Electrochem.*, 2014, vol. 50, no. 1, pp. 9–17.

16. Belevskii, S.S., Buravets, V.A., Yushchenko, S.P., et al., *Surf. Eng. Appl. Electrochem.*, 2016, vol. 52, no. 4, pp. 350–355.

Translated by A. Kukhauk